Irregular Repetition Slotted ALOHA with Multi-Antenna Reception over Rayleigh Block Fading Channels

Yuhei Takahashi*, Daiki Fukui*, Guanghui Song†, Tomotaka Kimura*, Zilong Liu‡, and Jun Cheng*
* Department of Intelligent Information Engineering and Sciences, Doshisha University, Kyoto, 610-0321, Japan
(e-mail: {cyjk1101, ctwk0108}@mail4.doshisha.ac.jp; tomkimur@mail.doshisha.ac.jp; jcheng@ieee.org)
† The State Key Laboratory of Integrated Services Networks, Xidian University, Xi'an 710071, China
(e-mail:songguanghui@xidian.edu.cn)
‡ School of Computer Science and Electronic Engineering, University of Essex, Colchester, CO4 3SQ, UK
(e-mail:zilong.liu@essex.ac.uk)

***Abstract*—We study irregular repetition slotted ALOHA (IR-SA) with multi-antenna reception over Rayleigh block fading channels. An exact closed-form expression for the average decoding error probability $\bar{\epsilon}_{m,L}$ is derived for collision sizes $m = 1$ and $m = 2$ by applying the inclusion–exclusion principle, which generalizes known single-antenna results and remains valid for any finite number of antennas. Using this result, we develop a density-evolution-based analysis of multi-antenna IR-SA systems and characterize belief-propagation (BP) thresholds. Numerical results for the corresponding maximum a posteriori (MAP) decoding thresholds and converse bounds are also presented, demonstrating threshold saturation with spatial coupling.**

***Index Terms*—Belief propagation threshold, irregular repetition slotted ALOHA, multi-antenna reception, random access, Rayleigh fading, successive interference cancellation.**

I. Introduction

Irregular repetition slotted ALOHA (IR-SA) [1]–[7] is a powerful random access protocol that enables reliable communication in massive machine-type networks through packet repetition and successive interference cancellation (SIC). In this paper, we consider an IR-SA system with *multi-antenna reception*, where a large number of single-antenna devices communicates with a common access point (AP) equipped with L receive antennas over a slotted frame. The receiver performs iterative *spatio-temporal* SIC across antennas and slots, whereby the system performance is characterized in the asymptotic regime by the maximum normalized offered traffic that can be reliably supported.

For Rayleigh block fading channels with single-antenna reception ($L = 1$), the decoding process within a slot can be accurately characterized using threshold-based decoding with intra-slot SIC. Here m represents the number of packets colliding within a slot, and an exact closed-form expression for the average decoding error probability $\bar{\epsilon}_{m,1}$ in the presence of $m-1$ interferers is available [1], [2], which enables a rigorous density evolution (DE)-based analysis of IR-SA systems.

However, extending this analytical framework to multi-antenna reception ($L > 1$) is nontrivial, since the signal-to-interference-plus-noise ratio (SINR) statistics and decoding events become significantly more complex. As a result, existing analyses of multi-antenna IR-SA systems largely rely on simplified packet-erasure models [8]–[10] or numerical simulations [11], and an exact closed-form expression of the decoding error probability is missing. Note that Srivatsa *et al.* [12, Theorem 3] derived an expression for the average successful decoding probability $\theta_m = 1 - \bar{\epsilon}_{m,L\to\infty}$ under maximal-ratio-combining-based SIC (MRC-SIC). However, their result relies on an approximation and does not provide a closed-form expression for finite L.

In this paper, we derive an exact closed-form expression for the average decoding error probability $\bar{\epsilon}_{m,L}$ (for $m = 1$ and $m = 2$) for IR-SA systems with L-antenna reception over Rayleigh fading channels. Our analysis considers selection-combining-based SIC (SC-SIC), in which the receiver selects the strongest signal among the L antennas. By applying the inclusion-exclusion principle, we characterize the average decoding error probabilities under intra-slot SIC in the presence of antenna diversity. This result generalizes the known single-antenna expression $\bar{\epsilon}_{m,1}$ and enables a rigorous DE-based analysis of multi-antenna IR-SA systems, leading to the derivation of belief-propagation (BP) thresholds.

Once DE is characterized, the converse bound and the maximum a posteriori (MAP) decoding threshold can be derived via extrinsic information transfer (EXIT) chart area arguments [3], [13], [14]. Prior works on MAP thresholds and converse bounds have primarily focused on either collision-channel models [3], [13], [15] or single-antenna Rayleigh fading scenarios [2], [7]. In contrast, this paper addresses the MAP threshold and the converse bound for IR-SA systems with *multi-antenna reception over Rayleigh fading channels*.

II. System model

A. IR-SA Access Protocol with Multi-Antenna Reception

We consider an IR-SA system with multi-antenna reception, where N_{T} single-antenna devices communicate with a common AP equipped with L antennas over a frame of M time slots. Let $\mathcal{L} = \{1, 2, \ldots, L\}$ denote the set of antenna

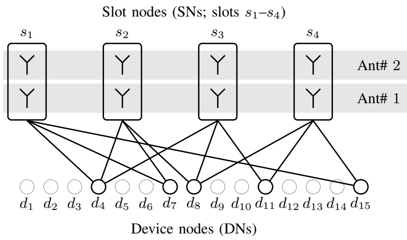

Fig. 1. Bipartite graph representation of multi-antenna IR-SA with $L = 2$, $M = 4$, $N_\mathrm{T} = 15$, $N_\mathrm{a} = 5$, and $\pi = N_\mathrm{a}/N_\mathrm{T} = 1/3$.

indices. The antennas at the AP are spaced sufficiently far apart to ensure independent fading values. In each frame, each device becomes active independently with probability $\pi \ll 1$ and, if active, generates one message that is encoded into a codeword (called a packet) using a common code $\mathcal{C}$ with code rate R. This encoder is implemented as a concatenation of a channel encoder and a higher-order modulator. We restrict our analysis to $R \geq 1$; the case $R < 1$ is discussed in [16]. Each active device selects a repetition degree l with probability Λ_l according to the distribution $\{\Lambda_l\}_{l=1}^{l_{\max}}$. It then transmits l replicas of its packet in l randomly selected slots within a frame.

We define the normalized population size as $\alpha \triangleq N_\mathrm{T}/M$, which is constant. The average normalized offered traffic is $G = \pi N_\mathrm{T}/M = \pi\alpha$, representing the average number of packets transmitted per slot when the packet loss rate (PLR) is lower than a target value. We are interested in the asymptotic ($M \to \infty$) traffic G, which depends on probability distribution $\{\Lambda_l\}_{l=1}^{l_{\max}}$, given the average received signal-to-noise ratio (SNR), the code rate R and the number of antennas L.

B. Bipartite Graph and Degree Distributions

As illustrated in Fig. 1, the multi-antenna IR-SA protocol outlined in Sec. II-A can be characterized in a manner analogous to conventional single-antenna IR-SA [4], [5]. Specifically, it is modeled as a bipartite graph $\mathcal{G} = (\mathcal{D}, \mathcal{S}, \mathcal{E})$. Here, $\mathcal{D}$ denotes the set of N_T device nodes (DNs), $\mathcal{S}$ denotes the set of M slot nodes (SNs), and $\mathcal{E}$ represents the set of edges. An edge connects a DN $d_i \in \mathcal{D}$ to an SN $s_j \in \mathcal{S}$ if and only if the i-th device selects the j-th slot for transmission.

Importantly, even with multiple receive antennas, all multi-antenna processing, including intra- and inter-antenna SIC, is encapsulated within each slot node. As a result, the bipartite graph structure depends only on device transmission patterns and remains identical to that of the single-antenna case, consistent with prior work [12]. Consequently, multi-antenna effects enter the DE-based analysis solely through the slot-node decoding success probability $(1 - \bar{\epsilon}_{m,L})$ (see (10)).

The number of edges connected to a DN or SN is defined as the node degree. In this framework, a DN has degree l (i.e., it has l edges connected to SNs) with probability Λ_l. The set $\{\Lambda_l\}_{l=1}^{l_{\max}}$ is referred to as the DN degree distribution, where the average number of replicas per active device is given by

$$\bar{d} \triangleq \Lambda'(1) = \textstyle\sum_{l=1}^{l_{\max}} l\Lambda_l. \tag{1}$$

As $N_\mathrm{T} \to \infty$, the SN degree distribution is Poisson with $\Psi_n = \exp(-\alpha\bar{d})(\alpha\bar{d})^n/n!$ [4], [5].

The degree distributions are also defined from an edge-perspective in polynomials [5]: $\lambda(x) = \sum_{l=1}^{l_{\max}} \lambda_l x^{l-1}$ with $\lambda_l = \frac{l\Lambda_l}{\sum_{l=1}^{l_{\max}} l\Lambda_l}$ and

$$\rho(x) = \textstyle\sum_{n=1}^{N_\mathrm{T}} \rho_n x^{n-1} = \exp(-\alpha\bar{d}(1-x)), \tag{2}$$

with Poisson distribution

$$\rho_n = \frac{n\Psi_n}{\sum_{n=1}^{N_\mathrm{T}} n\Psi_n} = \exp(-\alpha\bar{d})\frac{(\alpha\bar{d})^{n-1}}{(n-1)!},\ n = 1, 2, \ldots. \tag{3}$$

C. Spatio-Temporal SIC Decoding in Rayleigh Block Fading

Decoding at the AP is an iterative decoding process, integrating both intra- and inter-slot as well as intra- and inter-antenna SICs.

1) Intra-Slot SIC: Assuming m packet replica collisions, the resultant L superimposed signals (one per antenna) within the slot are given by

$$\boldsymbol{y}_i = \textstyle\sum_{k\in\mathcal{K}} h_{k,i}\boldsymbol{x}_k + \boldsymbol{z}_i, \quad i = 1, 2, \ldots, L, \tag{4}$$

where $\mathcal{K}$ ($|\mathcal{K}| = m$) is the set of active devices. Here, device k is active and has accessed the slot. The vector $\boldsymbol{x}_k \in \mathcal{C}$ represents its codeword (or packet) of code $\mathcal{C}$. The vector $\boldsymbol{z}_i \sim \mathcal{CN}(\mathbf{0}, \sigma^2 I)$ is an additive circularly symmetric complex Gaussian (CSCG) noise with mean $\mathbf{0}$ and diagonal covariance matrix $\sigma^2 I$ with noise power σ^2 and identity matrix I.

The channel coefficient $h_{k,i}$ expresses the fading of the channel from the active device k to Ant# i of AP during the slot, which remains constant within a slot and varies independently across slots. For Rayleigh block fading channels, the received SNR $\gamma_{k,i} \triangleq P|h_{k,i}|^2/\sigma^2$ is exponentially distributed with $p_\gamma(x) = 1/\bar{\gamma}\cdot e^{-\frac{x}{\bar{\gamma}}},\ x > 0$, where $\bar{\gamma}$ is the average received SNR.

Decoding at AP within a slot involves an iterative process alternating between intra-antenna and inter-antenna SICs. It is assumed that the AP has full knowledge of the channel state information (CSI) and the number of packet collisions. We consider SC-SIC, in which SIC is performed independently at each antenna, and the antenna branch with the strongest received signal is selected for packet decoding.

a) Intra-Antenna SIC: Assuming an m-packet collision, at Ant# i, the SINR of the packet from device k, assuming $\gamma_{1,i} > \gamma_{2,i} > \cdots > \gamma_{m,i}$, can be calculated as

$$\eta_{k,i} \triangleq \frac{P|h_{k,i}|^2}{\sigma^2 + \sum_{u=k+1}^{m} P|h_{u,i}|^2} = \frac{\gamma_{k,i}}{1 + \sum_{u=k+1}^{m}\gamma_{u,i}}. \tag{5}$$

Assuming threshold-based decoding, the packet $\boldsymbol{x}_k$ is successfully decoded if the SINR $\eta_{k,i}$ exceeds the threshold η_0, i.e.,

$$\Pr\{\text{packet } \boldsymbol{x}_k \text{ decoded}\} = \begin{cases} 1, & \eta_{k,i} > \eta_0, \\ 0, & \eta_{k,i} \leq \eta_0, \end{cases} \tag{6}$$

where η_0 satisfies $R = \log_2(1 + \eta_0)$ for code $\mathcal{C}$ of rate R. Upon successful decoding, the packet is removed from the received signal $\boldsymbol{y}_i$. Subsequent decoding proceeds with the interference-removed signal. This iterative process is termed *intra-antenna* SIC.

Remark 1 (κ-MaxDecoding)**.** *Let κ denote the maximum number of colliding packets, either initial or residual, for which intra-antenna SIC is applied in a slot. Although intra-antenna SIC can be applied to collisions of arbitrary size due to the unbounded Poisson collision distribution, practical systems typically restrict SIC to low-order collisions because of interference, error propagation, and computational complexity [17]. Accordingly, we adopt the κ-MaxDecoding (e.g., $\kappa = 2$), in which intra-antenna SIC is performed only when the number of residual packets in a slot does not exceed κ. Hence, a slot originally containing an m-packet collision with $m > \kappa$ may still be decoded after inter-slot SIC if the residual degree is at most κ.* □

An undecoded packet $\boldsymbol{x}_k$ with SNR above η_0, i.e., $\gamma_{k,i} > \eta_0$, is termed a *potentially decodable (PD)* packet [18], because it can be decoded upon removing the interfering packet $\boldsymbol{x}_{j \neq k}$ from signal $\boldsymbol{y}_i$.

b) Inter-Antenna SIC: The previously described intra-antenna SIC process enables the successful decoding of packets. These decoded packets are then canceled from the receive signals of other antennas within the same slot. This procedure is referred to as *inter-antenna* SIC.

The above two processes are repeated across all antenna elements until no further decoding is possible for any packet at any antenna element. This iterative decoding procedure is referred to as *intra-slot* SIC due to its execution within a slot.

2) Inter-Slot SIC: Following intra-slot SIC, once packets are successfully decoded, their replicas are removed from the specific slots identified by those packets. This processing, termed *inter-slot SIC*, facilitates subsequent intra-slot SIC on the remaining signals in those slots.

The intra- and inter-slot SIC processes can be modeled as the successive removal of edges in a bipartite graph $\mathcal{G}$. When a packet from a device (or a DN) is successfully decoded at at least one antenna in a slot (or a SN), the corresponding edge connected to the SN is removed via intra-slot SIC. Subsequently, all l edges incident to the same DN are removed through inter-slot SIC. This process iterates until no further edges can be eliminated.

III. Average Error Probability within a Slot

Consider a generic slot t with m packets received by L antennas, as in (4), and select one packet as the reference. We derive closed-form expressions for $\bar{\epsilon}_{m,L}$ for $m = 1, 2$ under intra-slot SIC performed across and within antennas. These results form the analytical basis for the DE framework developed in the next section.

In threshold-based decoding, a single decoding step is defined as the recovery of a packet at any of the L antennas, followed by its cancellation from all antennas. Consequently, for an m-collision, up to m successive steps may be required. Let $D(m, r, L)$ denote the probability that the reference packet is successfully decoded specifically at step r. The average decoding error probability for the reference packet in the presence of $m-1$ interferers within a slot using L antennas is

$$\bar{\epsilon}_{m,L} = 1 - \textstyle\sum_{r=1}^{m} D(m, r, L). \quad (7)$$

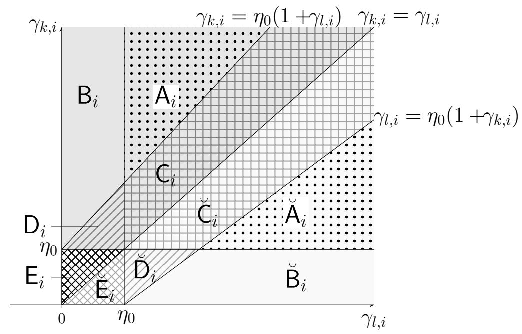

Fig. 2. The SIC feasible region in a two-collision within a slot ($R \geq 1$).

TABLE I
Events at a single antenna, where P_k and P_l are packets sent by device k and l, respectively.

region	event
A ($\breve{\mathsf{A}}$)	P_k (P_l) is decoded first and then P_l (P_k) is decoded.
B ($\breve{\mathsf{B}}$)	P_k (P_l) is decoded, while P_l (P_k) is undecoded and PD.
C, $\breve{\mathsf{C}}$	P_k and P_l are PD.
D ($\breve{\mathsf{D}}$)	P_k (P_l) is undecoded and PD; P_l (P_k) is undecoded and not PD.
E, $\breve{\mathsf{E}}$	P_k and P_l are undecoded and not PD.

Before proceeding, Table I summarizes the probabilities of the possible events for the single-antenna case. The received SNRs from devices k and l at Ant# i are denoted by $\gamma_{k,i}$ and $\gamma_{l,i}$, respectively. The random variables (RVs) $\gamma_{k,i}$, $\gamma_{l,i}$, $\gamma_{k,j}$, and $\gamma_{l,j}$ ($k, l \in \mathcal{D}$, $k \neq l$ and $i, j \in \mathcal{L}$, $i \neq j$) are mutually independent. The integral regions illustrated in Fig. 2 are introduced to clarify the computation. For example, the probability associated with the region A_i is denoted as P_{A_i}. Due to symmetry, we have $P_{\Gamma_i} = P_{\breve{\Gamma}_i} \triangleq P_{\Gamma}$, $\Gamma \in \{\mathsf{A}, \mathsf{B}, \mathsf{C}, \mathsf{D}, \mathsf{E}\}$. The extended version of this paper [16] provides the closed-form expressions for these probabilities, which serve as the basis for the calculations in the L-antenna case.

In deriving the results for the L-antenna case, we rely on the following fundamental facts:

(i) RVs $\gamma_{k,i}$ are independent and identically distributed.
(ii) The inclusion-exclusion principle for computing the probability of the union of L sets $A_1, \ldots, A_L$ [19]:

$$\Pr(\cup_{\ell=1}^{L} A_\ell) = \sum_{\emptyset \neq \mathcal{S} \subseteq \{1,\ldots,L\}} (-1)^{|\mathcal{S}|+1} \Pr(\cap_{\ell \in \mathcal{S}} A_\ell). \quad (8)$$

A. Closed-form Expression for a Single-Packet Slot ($m = 1$)

The probability that the packet of device k, which is the only packet received in the slot, is successfully decoded by at least one of the antennas, is given by

$$D(1, 1, L) = 1 - \prod_{i=1}^{L} (1 - \Pr\{\gamma_{k,i} > \eta_0\}) = 1 - (1 - e^{-\frac{\eta_0}{\bar{\gamma}}})^L.$$

B. Closed-form Expression for a Two-Collision Slot ($m = 2$)

1) $D(2,1,L)$: We derive the probability that the reference packet is successfully decoded in the first threshold-based decoding step. This probability is expressed as

$$D(2,1,L) = \frac{1}{2}\Pr\{\varUpsilon\} = \frac{1}{2}\left(\sum_{\ell=1}^{L}(-1)^{\ell+1}\binom{L}{\ell}\{2(P_{\mathsf{A}}+P_{\mathsf{B}})\}^{\ell}\right).$$

Here, $\Pr\{\varUpsilon\}$ denotes the probability that either P_k or P_l is decodable at any of the L antennas in the first step. Note that the reference packet is either P_k or P_l with probability $1/2$. The detailed derivations can be found in [16] and are omitted here due to space limitations.

2) $D(2,2,L)$: Next, we derive the probability that the reference packet is successfully decoded in the second threshold-based decoding step. This probability is expressed as

$$D(2,2,L) = \big(\Pr\{\varDelta\} + \Pr\{\varXi\}\big)/2.$$

Here, $\Pr\{\varDelta\}$ denotes the probability that two packets are decoded at the same antenna in $\mathcal{L}$. In contrast, $\Pr\{\varXi\}$ represents the probability that the packets are successfully decoded across at least two distinct antennas. This probability is derived by considering all possible antenna combinations for two scenarios: 1) P_l and P_k are decoded independently at distinct antennas, respectively; and 2) the initial decoding of P_l (P_k) in an antenna set $\mathcal{L}_1 \subset \mathcal{L}$ with $|\mathcal{L}_1| = \ell_1$ and its subsequent cancellation via inter-antenna SIC enables the decoding of P_k (P_l) in a distinct set $\mathcal{L}_2 \subset \mathcal{L} \setminus \mathcal{L}_1$ with $|\mathcal{L}_2| = \ell_2$. Moreover, the reference packet decoded in the second step is either P_k or P_l with probability $1/2$.

Using the inclusion-exclusion principle (8), we obtain [16]

$$\Pr\{\varDelta\} = \sum_{\ell=1}^{L}(-1)^{\ell+1}\binom{L}{\ell}(2P_{\mathsf{A}})^{\ell},$$

$$\Pr\{\varXi\} = \sum_{\ell_1=1}^{L-1}\sum_{\ell_2=1}^{L-\ell_1}(-1)^{\ell_1+\ell_2}\binom{L}{\ell_1}\binom{L-\ell_1}{\ell_2}\xi_{\varXi}(\ell_1,\ell_2),$$

where

$$\xi_{\varXi}(\ell_1,\ell_2) = (2P_{\mathsf{B}}^{\ell_1}(P_{\mathsf{B}}+2P_{\mathsf{C}}+P_{\mathsf{D}})^{\ell_2} - P_{\mathsf{B}}^{\ell_1+\ell_2})(1-2P_{\mathsf{A}})^{L-\ell_1-\ell_2}.$$

Remark 2. *Focusing on the case $m = 2$, the average decoding error probability $\bar{\epsilon}_{m,L}$ for MRC-SIC in [12, Theorem 3] is obtained via an approximation that is accurate only in the large-L regime. In contrast, the proposed SC-SIC scheme provides an exact closed-form expression for $\bar{\epsilon}_{m,L}$ that is valid for any finite L. As shown in Table II, the SC-SIC analytical results closely match the simulation results for all considered finite L, while the MRC-SIC approximation exhibits a noticeable mismatch.* □

TABLE II
AVERAGE DECODING ERROR PROBABILITY $\bar{\epsilon}_{m,L}$ ($m = 1, 2$) WITHIN A SLOT. Gap DENOTES THE ABSOLUTE DIFFERENCE $|\text{Sim.} - \text{Theo.}|$. SIMULATION RESULTS REPORTED AS $< 10^{-6}$ INDICATE THAT NO DECODING ERROR WAS OBSERVED OVER 10^6 MONTE-CARLO TRIALS. ($\eta_0 = 10, \bar{\gamma} = 10$ dB).

		MRC-SIC [12, Theorem 3]			SC-SIC (7)		
m	L	Sim.	Theo.	Gap	Sim.	Theo.	Gap
1	4	1.88×10^{-2}	1.90×10^{-2}	1.7×10^{-4}	1.60×10^{-1}	1.60×10^{-1}	1.0×10^{-4}
	8	1.0×10^{-5}	1.0×10^{-5}	$< 10^{-6}$	2.53×10^{-2}	2.55×10^{-2}	2.0×10^{-4}
	16	$< 10^{-6}$	$< 10^{-6}$	$< 10^{-6}$	7.0×10^{-4}	7.2×10^{-4}	1.8×10^{-5}
	32	$< 10^{-6}$	$< 10^{-6}$	$< 10^{-6}$	$< 10^{-6}$	4.2×10^{-7}	4.2×10^{-7}
	64	$< 10^{-6}$	$< 10^{-6}$	$< 10^{-6}$	$< 10^{-6}$	1.8×10^{-13}	1.8×10^{-13}
2	4	6.16×10^{-1}	7.32×10^{-1}	1.2×10^{-1}	7.89×10^{-1}	7.89×10^{-1}	5.1×10^{-5}
	8	3.68×10^{-1}	4.81×10^{-1}	1.1×10^{-1}	5.84×10^{-1}	5.84×10^{-1}	9.7×10^{-5}
	16	1.41×10^{-1}	2.07×10^{-1}	6.6×10^{-2}	3.31×10^{-1}	3.31×10^{-1}	1.7×10^{-4}
	32	2.25×10^{-2}	3.84×10^{-2}	1.6×10^{-2}	1.10×10^{-1}	1.09×10^{-1}	3.9×10^{-4}
	64	7.0×10^{-4}	1.3×10^{-3}	6.0×10^{-4}	1.19×10^{-2}	1.19×10^{-2}	3.1×10^{-5}

IV. DENSITY EVOLUTION WITH L-ANTENNA RECEPTION

In this section, building on [1], [2], [4] and the closed-form results of the previous section, we derive two DE iteration equations that characterize the asymptotic performance ($M, N_{\mathrm{T}} \to \infty$) of multi-antenna IR-SA systems.

We refer to the DNs (SNs) as the DN (SN) group. In the protograph, let ${}^{\ell}p$ be the probability that an edge incident on the DN group carries an erasure message towards SNs for the ℓ-th iteration. Similarly, let ${}^{\ell}q$ be the probability that an edge incident on the SN group carries an erasure message towards the DN groups.

First, consider the DN group, which has degree distribution $\lambda(x)$. In the ℓ-th iteration, an edge incident to a degree-l DN is removed if at least one of the other $l-1$ edges has been successfully resolved. Given the device activation probability π, the average probability that a DN-to-SN message remains erased is expressed as [2]–[4]:

$$ {}^{\ell}p = \pi \textstyle\sum_{l=1}^{l_{\max}} \lambda_l \cdot {}^{(\ell-1)}q^{l-1} = \pi\lambda({}^{(\ell-1)}q). \quad (9)$$

Second, consider the SN group, which has degree distribution $\rho(x)$. The probability that an edge carries an erasure message from the SN group to the DN group in the ℓ-th iteration is ${}^{\ell}q = \sum_{r=1}^{\infty}\rho_r \cdot {}^{\ell}q^{(r)}$. Here ρ_r is the fraction of edges connected to an SN of degree-r (see (3)), and ${}^{\ell}q^{(r)}$ is the probability that an edge carries an erasure message, given that it is connected to the SN of degree-r. The erasure probability of the degree-r SN is [2]

$$ {}^{\ell}q^{(r)} = 1 - \textstyle\sum_{m=1}^{r}\binom{r-1}{m-1}(1-{}^{\ell}p)^{r-m}({}^{\ell}p)^{m-1}(1-\bar{\epsilon}_{m,L}). \quad (10)$$

Here, $(1-\bar{\epsilon}_{m,L})$ denotes the probability that the replica associated with an outgoing edge is successfully decoded when the reduced degree of the SN is m. In other words, in a slot where r replicas collide, $r-m$ replicas are removed via inter-slot SIC, after which the receiver attempts to decode a randomly selected replica among the remaining m replicas using L receive antennas. The closed-form expression of $\bar{\epsilon}_{m,L}$ is provided in Sec. III.

With some manipulations, we have [1], [2]

$$ {}^{\ell}q = 1 - e^{-\alpha\bar{d}\,{}^{\ell}p}\textstyle\sum_{m=0}^{\infty}\frac{(\alpha\bar{d}\,{}^{\ell}p)^m}{m!}(1-\bar{\epsilon}_{m+1,L}). \quad (11)$$

Substituting for (9) with $G = \pi\alpha$, we have, with ${}^{(\ell=0)}q = 1$,

$$ {}^{\ell}q = 1 - e^{-G\bar{d}\lambda({}^{(\ell-1)}q)}\sum_{m=0}^{\infty}\frac{(G\bar{d}\lambda({}^{(\ell-1)}q))^m}{m!}(1-\bar{\epsilon}_{m+1,L}). \quad (12)$$

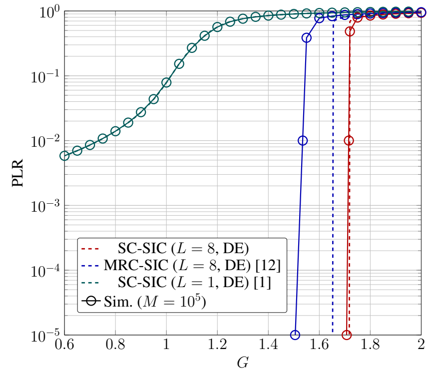

Fig. 3. PLRs vs. offered traffic G of IR-SA for the MRC-SIC [12] and the proposed SC-SIC: $\eta_0 = 5$, $\bar{\gamma} = 20$ dB, and $\Lambda(x) = 0.586x^2 + 0.291x^3 + 0.031x^6 + 0.022x^7 + 0.006x^8 + 0.063x^{10}$.

Let ${}^{(\infty)}q(G, \bar{d}, L, \bar{\gamma}, \eta_0) = \lim_\ell {}^{(\ell)}q$ be the convergence value of the iteration. The PLR of the systems is [1], [4]

$$\begin{aligned}\mathrm{PLR}(G, \bar{d}, L, \bar{\gamma}, \eta_0) &= \Lambda({}^{(\infty)}q(G, \bar{d}, L, \bar{\gamma}, \eta_0)) \\ &= \sum_{l=1}^{l_{\max}} \Lambda_l \left({}^{(\infty)}q(G, \bar{d}, L, \bar{\gamma}, \eta_0)\right)^l . \quad (13)\end{aligned}$$

Given target PLR*, the asymptotic iterative decoding threshold, also called the BP decoding threshold, is defined as the supremum offered traffic value [4] [1]:

$$G^{\mathrm{BP,blk}} = \sup\{G : \mathrm{PLR}(G, \bar{d}, L, \bar{\gamma}, \eta_0) \to 0\}. \quad (14)$$

Under the κ-MaxDecoding in Remark 1, the summation in (12) is restricted to residual degrees $m \le \kappa - 1$ (e.g., $\kappa = 2$).

V. Numerical and Simulation Results

In this section, using the closed-form expressions of $\bar{\epsilon}_{m,L}$ and DE under the ($\kappa = 2$)-MaxDecoding assumption, we present numerical results for the BP thresholds in (14), along with the corresponding MAP thresholds and converse bounds. The derivations of the MAP thresholds and converse bounds are omitted due to space limitations and can be found in [16].

Figure 3 compares the PLR performance of multi-antenna IR-SA using the MRC-SIC and our proposed SC-SIC (13) for $L = 8$ at a target PLR$^* = 10^{-2}$. For reference, the performance of the single-antenna IR-SA ($L = 1$) [1] is also included. The same degree distribution, optimized specifically for the proposed multi-antenna IR-SA via a differential evolution algorithm [20], is applied to all schemes. Simulation results with a finite number of slots ($M = 10^5$) for SC-SIC closely match the asymptotic DE analysis, thereby validating our analytical framework; the small residual gap is attributable to the finite number of slots in the simulation. In contrast, the MRC-SIC approach in [12] exhibits a noticeable discrepancy between simulation and analysis. This is because its analysis is approximate for $m \ge 2$, as indicated by the results in Table II.

Figure 4 plots the BP thresholds $G^{\mathrm{BP,blk}}$ versus the average received SNR $\bar{\gamma}$ for $L = 8$ and 16. At low SNRs ($\bar{\gamma} < 12$ dB), MRC-SIC achieves higher BP thresholds due to its combining gain, which is essential for raising the effective SNR above the decoding threshold η_0. By contrast, the lack of combining

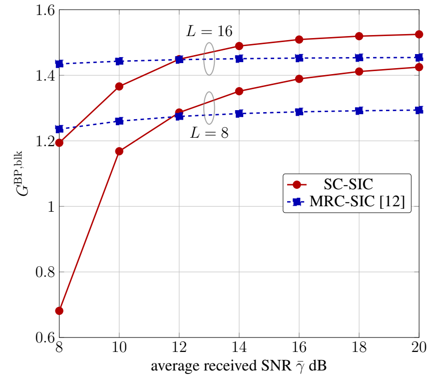

Fig. 4. BP thresholds $G^{\mathrm{BP,blk}}$ vs. average received SNR $\bar{\gamma}$ for MRC-SIC [12] and SC-SIC; $\Lambda(x) = x^3$, $\eta_0 = 10$, and $L = 8, 16$.

TABLE III
BP thresholds of the spatially coupled scheme, $G^{\dagger\mathrm{BP,Conv}}$, MAP thresholds of d-regular repetition SA, $G^{\mathrm{MAP,blk}}_{\mathrm{reg}}$, and IR-SA, $G^{\mathrm{MAP,blk}}$, as well as the converse bound $G^{\mathrm{C,blk}}$ ($\eta_0 = 1, \bar{\gamma} = 20$ dB).

L	$\bar{d}$, (d)	$G^{\dagger\mathrm{BP,Conv}}$	$G^{\mathrm{MAP,blk}}_{\mathrm{reg}}$	$G^{\mathrm{MAP,blk}}$	$G^{\mathrm{C,blk}}$
1 [2]	3.103 (3)	1.824	1.824	1.826	1.829
2	3.066 (3)	1.969	1.969	1.969	1.972
3	3.068 (3)	1.976	1.976	1.976	1.979

gain in SC-SIC causes the SINRs across all L antennas to remain below the decoding threshold, thereby leading to a complete decoding failure. At high SNRs ($\bar{\gamma} \ge 12$ dB), a performance crossover occurs. While intra-antenna SIC likely succeeds on at least one antenna even without combining, MRC-SIC indiscriminately aggregates interference from all antennas, thereby limiting the effective SINR.

Once the DE iterative equations are obtained, the MAP threshold and the converse bound for the L-antenna IR-SA can be evaluated [16]. Table III summarizes these thresholds and bounds. In addition, the L-antenna spatially coupled scheme [16], extended from the single-antenna case [2], [3], yields the BP thresholds $G^{\dagger\mathrm{BP,Conv}}$, demonstrating threshold saturation.

VI. Conclusion

This paper developed an analytical framework for IR-SA with multi-antenna reception over Rayleigh block fading channels. Exact closed-form expressions for the average decoding error probability $\bar{\epsilon}_{m,L}$ under SC-SIC enabled a rigorous DE analysis without altering the bipartite graph. The obtained BP and MAP thresholds, along with the converse bounds, demonstrated threshold saturation via spatial coupling and elucidated the performance trade-offs between SC-SIC and MRC-SIC. Future work will address higher-order collisions, alternative combining schemes, and more general fading models.

Acknowledgment

The work of Z. Liu was supported in part by the UK Engineering and Physical Sciences Research Council under Grant EP/Y000986/1 ('SORT').

References

[1] F. Clazzer, E. Paolini, I. Mambelli, and Č. Stefanović, "Irregular repetition slotted ALOHA over the Rayleigh block fading channel with capture," in *Proc. IEEE Int. Conf. Commun. (ICC)*, 2017, pp. 1–6.

[2] Y. Takahashi, G. Song, T. Kimura, and J. Cheng, "Irregular repetition slotted ALOHA over Rayleigh block fading channels: Bounds and threshold saturation via spatial coupling," *IEEE Access*, vol. 11, pp. 106 528–106 543, 2023.

[3] G. Liva, E. Paolini, M. Lentmaier, and M. Chiani, "Spatially-coupled random access on graphs," in *Proc. IEEE Int. Symp. Inf. Theory (ISIT)*, 2012, pp. 478–482.

[4] G. Liva, "Graph-based analysis and optimization of contention resolution diversity slotted ALOHA," *IEEE Trans. Commun.*, vol. 59, no. 2, pp. 477–487, 2011.

[5] E. Paolini, Č. Stefanović, G. Liva, and P. Popovski, "Coded random access: Applying codes on graphs to design random access protocols," *IEEE Commun. Mag.*, vol. 53, no. 6, pp. 144–150, 2015.

[6] G. Liva, E. Paolini, Č. Stefanović, and A. G. i Amat, "Coded slotted ALOHA over the on-off fading channel: Performance bounds," in *Proc. 53rd Asilomar Conf. Signals, Syst., Comput.*, 2019, pp. 31–35.

[7] Y. Takahashi, I. Masuo, G. Song, T. Kimura, and J. Cheng, "Coded slotted ALOHA over Rayleigh block fading channels: BP threshold and converse bound," in *Proc. 2023 IEEE Globecom Wkshps. (GC Wkshps.)*, 2023, pp. 1523–1528.

[8] D. Jakovetić, D. Bajović, D. Vukobratović, and V. Crnojević, "Cooperative slotted ALOHA for multi-base station systems," *IEEE Trans. Commun.*, vol. 63, no. 4, pp. 1443–1456, 2015.

[9] C.-H. Yu, L. Huang, C.-S. Chang, and D.-S. Lee, "Poisson receivers: A probabilistic framework for analyzing coded random access," *IEEE/ACM Trans. Netw.*, vol. 29, no. 2, pp. 862–875, 2021.

[10] E. Recayte and C. Amatetti, "Multi-satellite NOMA-irregular repetition slotted ALOHA for IoT networks," in *Proc. IEEE Int. Conf. Commun. (ICC)*, 2025, pp. 2024–5209.

[11] X. Li, L. Zhao, and T. Yang, "Pilot-free slotted ALOHA for massive access," *IEEE Trans. Veh. Technol.*, vol. 73, no. 9, pp. 13 903–13 908, 2024.

[12] C. R. Srivatsa and C. R. Murthy, "On the impact of channel estimation on the design and analysis of IRSA based systems," *IEEE Trans. Signal Process.*, vol. 70, pp. 4186–4200, 2022.

[13] E. Paolini, G. Liva, and M. Chiani, "Graph-based random access for the collision channel without feedback: Capacity bound," in *Proc. 2011 IEEE Global Telecommun. Conf. (GLOBECOM)*, 2011, pp. 1–5.

[14] A. Ashikhmin, G. Kramer, and S. ten Brink, "Extrinsic information transfer functions: Model and erasure channel properties," *IEEE Trans. Inf. Theory*, vol. 50, no. 11, pp. 2657–2673, 2004.

[15] E. Paolini, G. Liva, and M. Chiani, "Coded slotted ALOHA: A graph-based method for uncoordinated multiple access," *IEEE Trans. Inf. Theory*, vol. 61, no. 12, pp. 6815–6832, 2015.

[16] Y. Takahashi, D. Fukui, G. Song, T. Kimura, Z. Liu, and J. Cheng, "Irregular repetition slotted ALOHA with multi-antenna reception: BP, MAP thresholds, and Converse bound." [Online]. Available: https://github.com/yuhei-takahashi/MultiAntIRSA/blob/main/MultiAntIRSA.pdf

[17] N. Zhang, J. Wang, G. Kang, and Y. Liu, "Uplink nonorthogonal multiple access in 5G systems," *IEEE Commun. Lett.*, vol. 20, no. 3, pp. 458–461, 2016.

[18] Z. Zhang, Y. Li, G. Song, C. Yuen, and Y. L. Guan, "Random NOMA with cross-slot successive interference cancelation packet recovery," *IEEE Wireless Commun. Lett.*, vol. 9, no. 7, pp. 1065–1069, 2020.

[19] S. M. Ross, *A First Course in Probability*, 6th ed. Upper Saddle River, NJ, USA: Prentice Hall, 1998.

[20] R. Storn and K. Price, "Differential evolution–a simple and efficient heuristic for global optimization over continuous spaces," *J. Glob. Optim.*, vol. 11, no. 4, pp. 341–359, 1997.